

— Supplementary Information —

Quenching of Photoluminescence in a Zn-MOF Sensor by Nitroaromatic Molecules

S. Jensen,^{1,2} K. Tan,^{3,*} W. Lustig,^{4,*} D. Kilin,⁵ J. Li,⁴ Y. J. Chabal,³ and T. Thonhauser^{1,2,†}

¹*Department of Physics, Wake Forest University, Winston-Salem, NC 27109, USA*

²*Center for Functional Materials, Wake Forest University, Winston-Salem, NC 27109, USA*

³*Department of Materials Science and Engineering,
University of Texas at Dallas, Richardson, TX 75080, USA*

⁴*Department of Chemistry and Chemical Biology,
Rutgers University, Piscataway, NJ 08854, USA*

⁵*Department of Chemistry and Biochemistry, North Dakota State University, Fargo, ND 58108, USA*

(Dated: January 20, 2019)

I. HUANG-RHYS FACTORS

To ensure that the electronic coupling methodology outlined in the main manuscript is applicable to our systems of interest, we have to show that our approximation of using the ground-state MD trajectory is sufficient to describe the excited state. To this end, we use a measure of mean displacement, i.e. the Huang-Rhys parameter D , which must be less than one but preferably close to zero. A value near zero indicates that the ionic and electronic structure is not perturbed substantially upon an excitation. To calculate D , we excite an

electron from the HOMO to the LUMO in each system and obtain the excited state geometry, which is then projected onto the phonon modes of the system and the best match is chosen. From this, we find the displacement d of the atom which moves the most, the reduced mass $m = m_1 m_2 / (m_1 + m_2)$ (where m_1 is the mass of the vibrating atom and m_2 is the mass of its nearest neighbor), and ω_0 corresponding to the angular frequency of the matching phonon mode. D can then be calculated as $D = d^2 m \omega_0 / 2\hbar$, and we find $D = 0.24$ for RPM3-Zn and 0.06 for DNT+RPM3-Zn.

| Mode | DNT+RPM3-Zn [cm ⁻¹] | DNT [cm ⁻¹] | Exp. Shift [cm ⁻¹] | Calc. Shift [cm ⁻¹] |
|--|------------------------------------|----------------------------|-----------------------------------|------------------------------------|
| $\nu(\text{C-H})_{\text{phenyl ring}}$ | 3104 | 3106 | 2 | 3 |
| $\nu_{\text{as}}(\text{NO}_2)$ | 1517 | 1534 | 17 | 16 |
| $\nu_{\text{s}}(\text{NO}_2)$ | 1343 | 1348 | 5 | 6 |
| $\nu(\text{C-N})$ | 1152 | 1133 | -19 | -11 |
| $\delta(\text{NO}_2)$ | 916 | 913 | -3 | -4 |
| $\omega(\text{NO}_2)$ | 732 | 732 | 0 | -2 |

TABLE S1. Assigned experimental IR modes of DNT in Figs. 3 and S3. The shifts of DNT peaks due to the adsorption inside RPM3-Zn are shown alongside the corresponding calculated ones. Assignments are made with the help of our DFT calculations and in conjunction with Ref. [1].

| Mode | RPM3-Zn [cm ⁻¹] | DNT+RPM3-Zn [cm ⁻¹] |
|-------------------------------------|--------------------------------|------------------------------------|
| $\nu(\text{C=C})_{\text{bpee}}$ | 1639 | 1639 |
| $\nu(\text{C=C})_{\text{bpdc}}$ | 1621 | 1621 |
| $\nu(\text{C=C-H})_{\text{bpee}}^a$ | 1413 | 1413 |
| $\nu(\text{C=C-H})_{\text{bpee}}^b$ | 1261 | 1261 |
| $\nu(\text{C=C-H})_{\text{bpee}}^c$ | 1228 | 1228 |
| $\nu(\text{C=C-H})_{\text{bpee}}^d$ | 1212 | 1212 |
| $\nu(\text{C=C-H})_{\text{bpdc}}$ | 1175 | 1170 |
| $\nu(\text{C-O})_{\text{bpdc}}$ | 1353 | 1353 |

TABLE S2. Assigned experimental IR modes of the bpee and bpdc linkers in Figs. 3 and S3. Assignments are made with the help of our DFT calculations and in conjunction with Refs. [2-4].

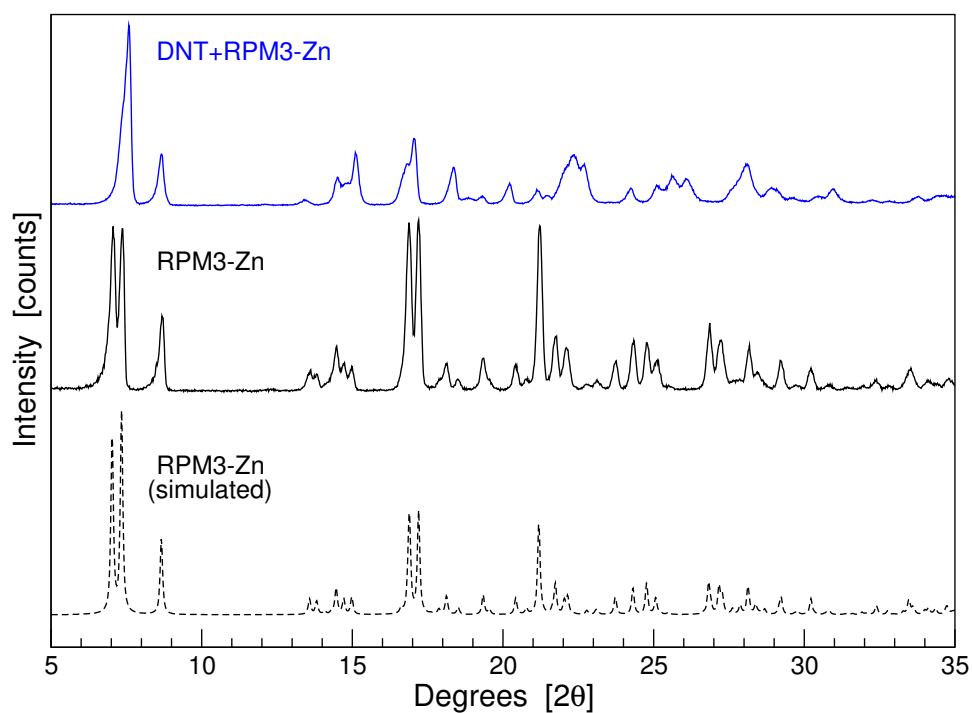


Figure S1. Powder X-ray diffraction (PXRD) patterns for samples of activated RPM3-Zn (black) and DNT+RPM3-Zn (blue) overlaid on the simulated PXRD pattern of RPM3-Zn (black dashed). All PXRD data was collected at room temperature on a Rigaku Ultima IV diffractometer using Cu $K\alpha$ radiation ($\lambda = 1.5406 \text{ \AA}$).

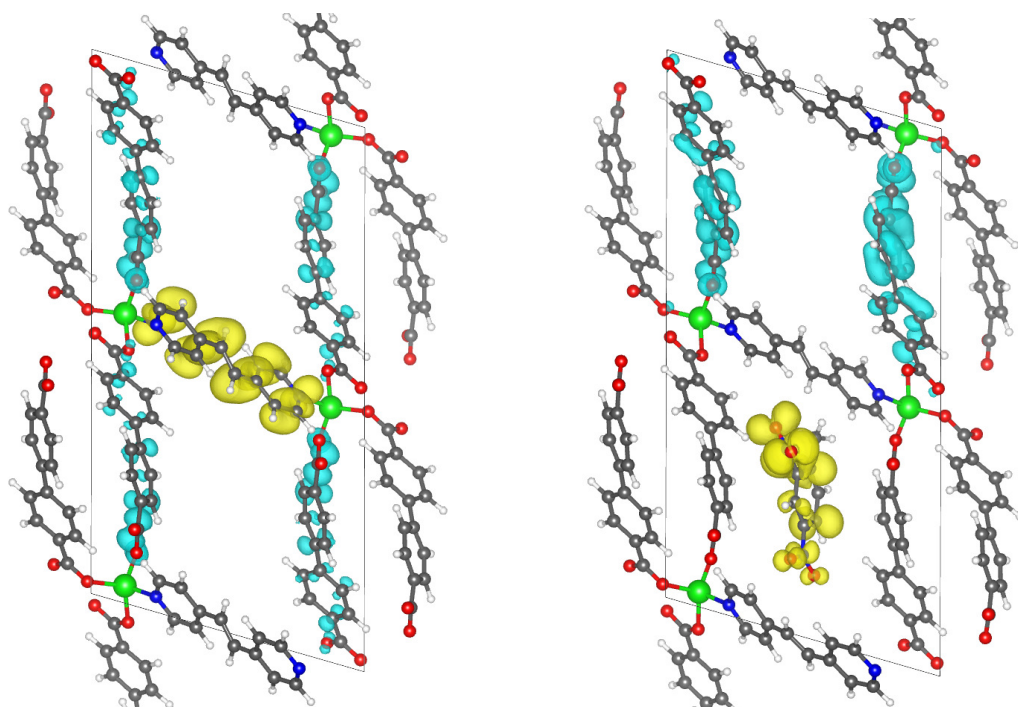


Figure S2. Band decomposed charge density images of RPM3-Zn (left) and DNT+RPM3-Zn (right). The HOMO is shown in blue and the LUMO is depicted in yellow, both at an isosurface value of $2 \times 10^{-3} e/\text{\AA}^3$. The adsorption of DNT shifts the LUMO away from the MOF linker to the guest molecule.

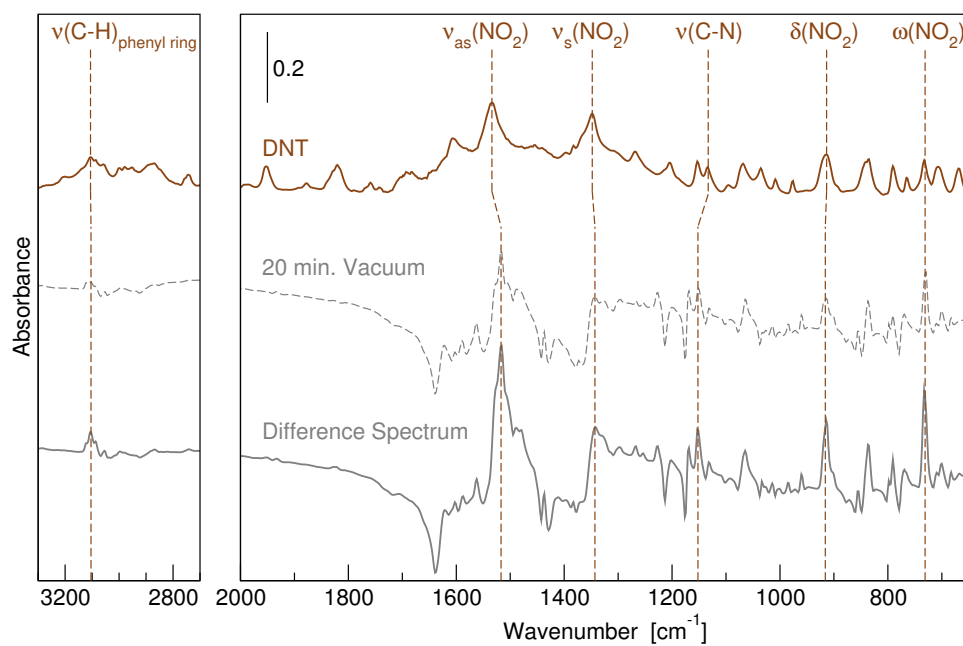


Figure S3. IR spectrum of DNT (brown) along with the IR difference spectrum between DNT+RPM3-Zn and RPM3-Zn (gray). The difference spectrum is also plotted after 20 minutes of evacuation (dashed).

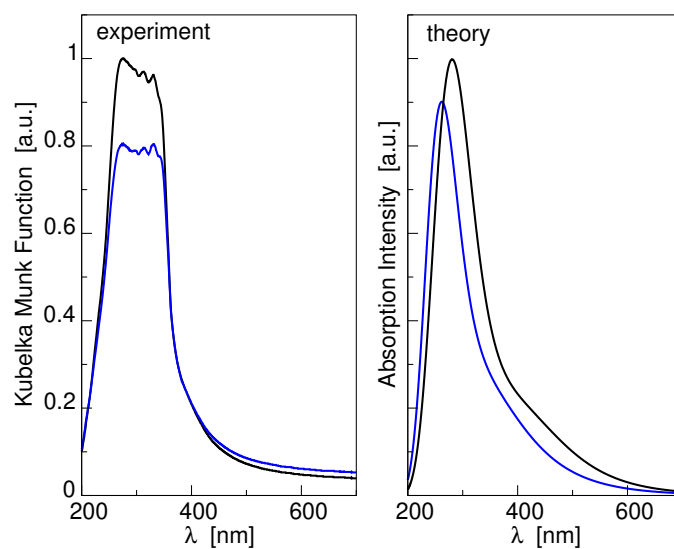


Figure S4. Experimental and computed RPM3-Zn (black) and DNT+RPM3-Zn (blue) absorption spectra. Both plots are normalized such that the RPM3-Zn peak height is 1. The computed spectra were calculated along the 1000 fs MD trajectory while the experimental spectra applied the Kubelka Munk equation to the reflectance data.

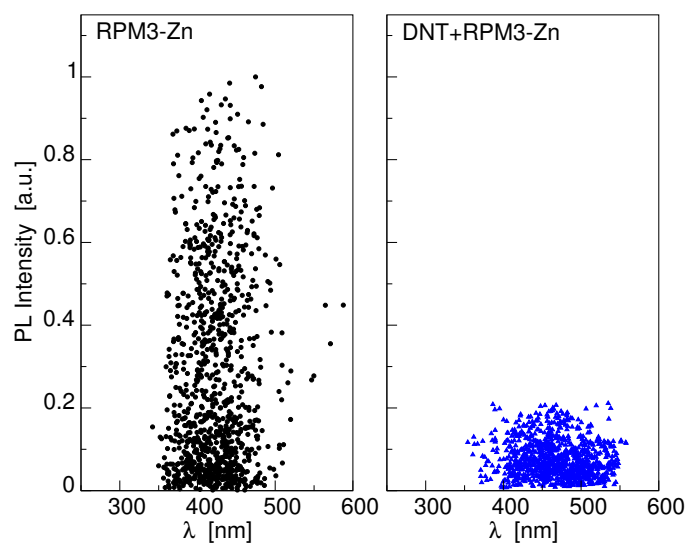


Figure S5. Plot of the RPM3-Zn and DNT+RPM3-Zn oscillator strengths at each time step along the 1000 time step MD trajectory. The quenching effect of DNT on the photoluminescence, as well as the observed emission red shift, is clearly visible.

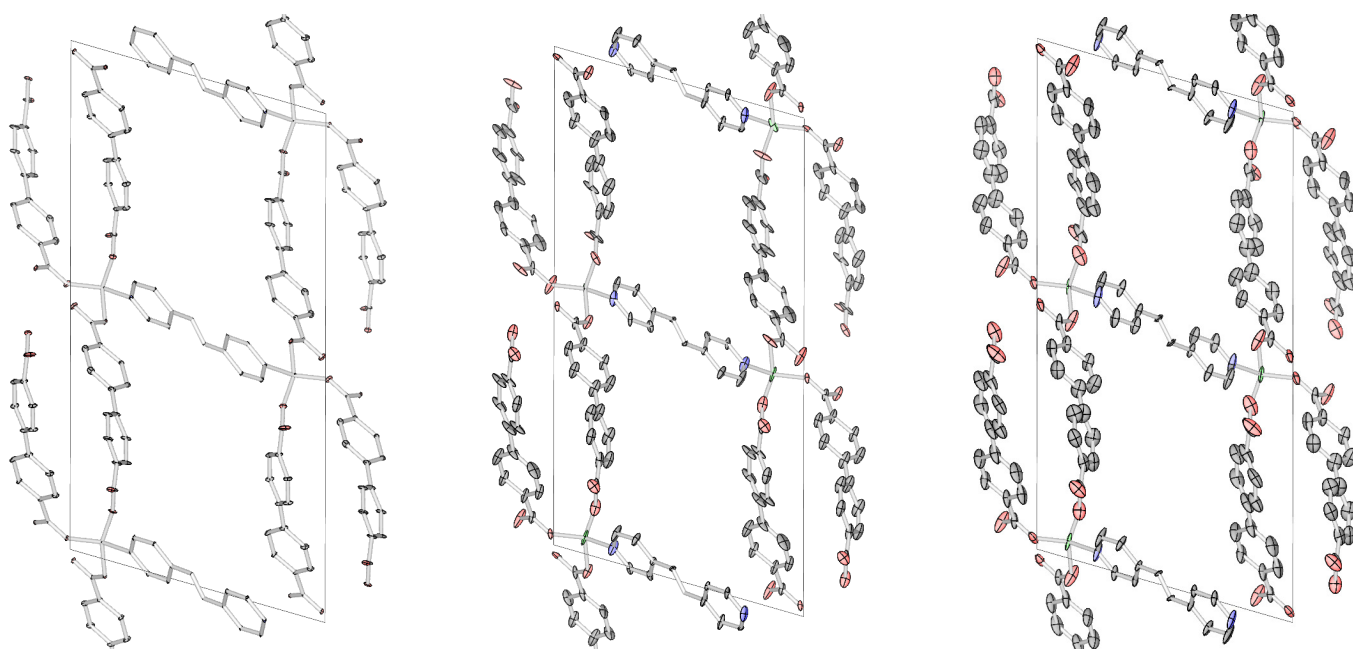


Figure S6. Thermal ellipsoid images of RPM3-Zn at $T = 50\text{ K}$ (left), $T = 300\text{ K}$ (middle), and $T = 550\text{ K}$ (right) at 99% probability. It is clear that increased temperature increases the amount of vibration, but the calculated oscillator strength values do not markedly decrease with increased vibration. The variance \mathbf{U} was calculated using the methods outlined under the Computational Details section. Thermal ellipsoids for hydrogen are not depicted for clarity.

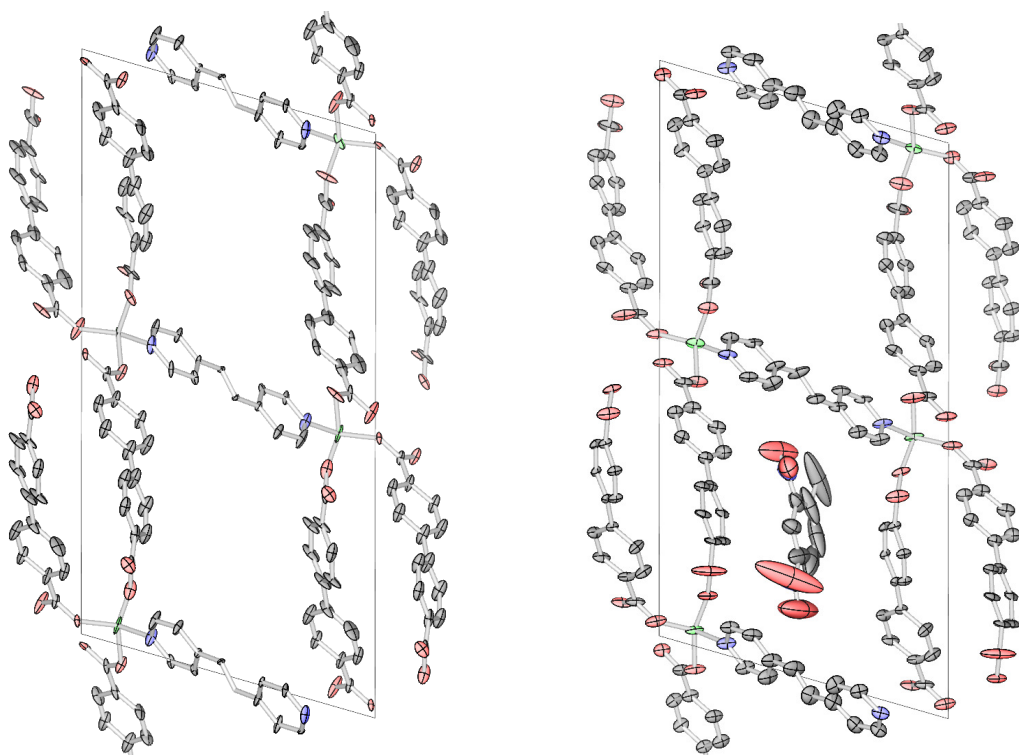


Figure S7. Thermal ellipsoid images of RPM3-Zn (left) and DNT+RPM3-Zn (right) at 99% probability for $T = 300\text{ K}$. The variance \mathbf{U} was calculated using the methods outlined under the Computational Details section. Thermal ellipsoids for hydrogen are not depicted for clarity.

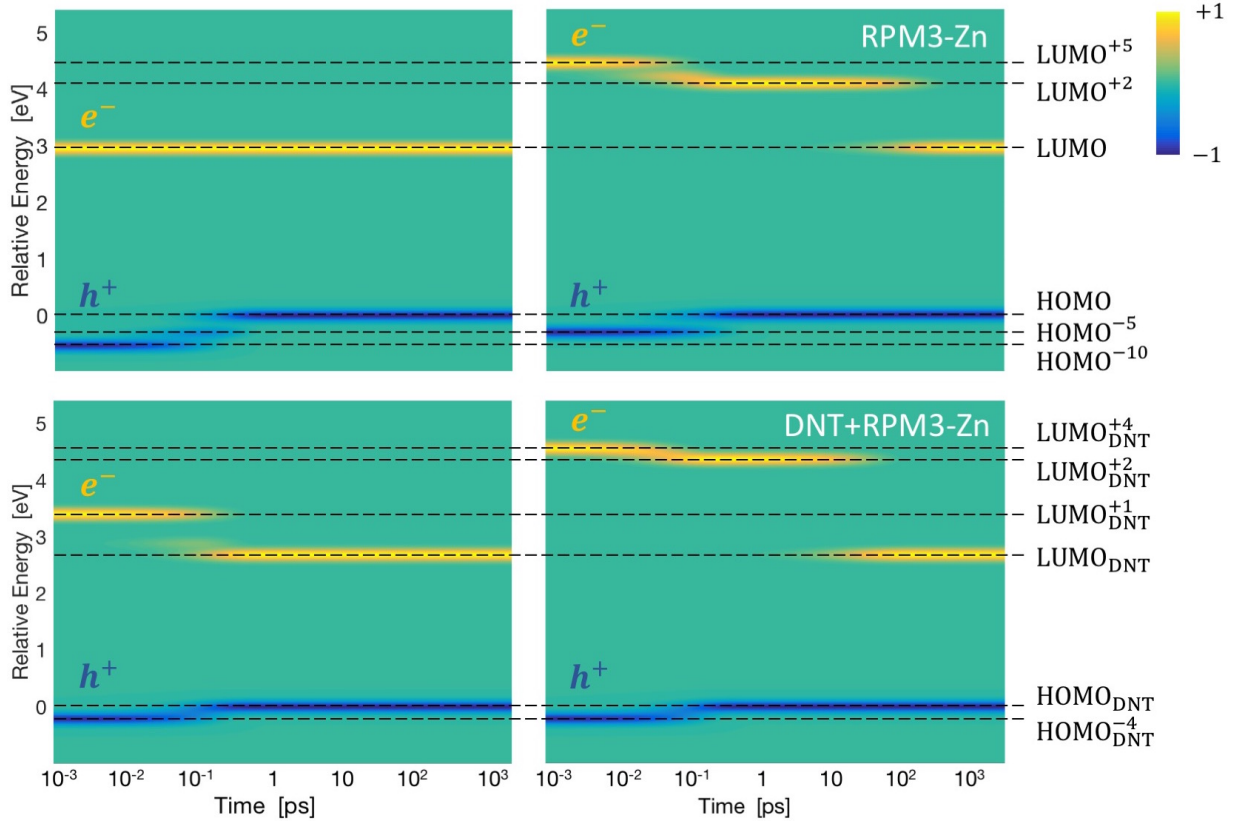


Figure S8. Electron and hole relaxation of RPM3-Zn (top) and DNT+RPM3-Zn (bottom) for a lower energy transition at 340 nm/3.65 eV (left) and a higher energy transition at 260 nm/4.77 eV (right). Yellow indicates a gain of an electron, blue indicates a loss of an electron (i.e. hole), and green indicates no change in charge. The corresponding real-space relaxations can be found in Fig. S9.

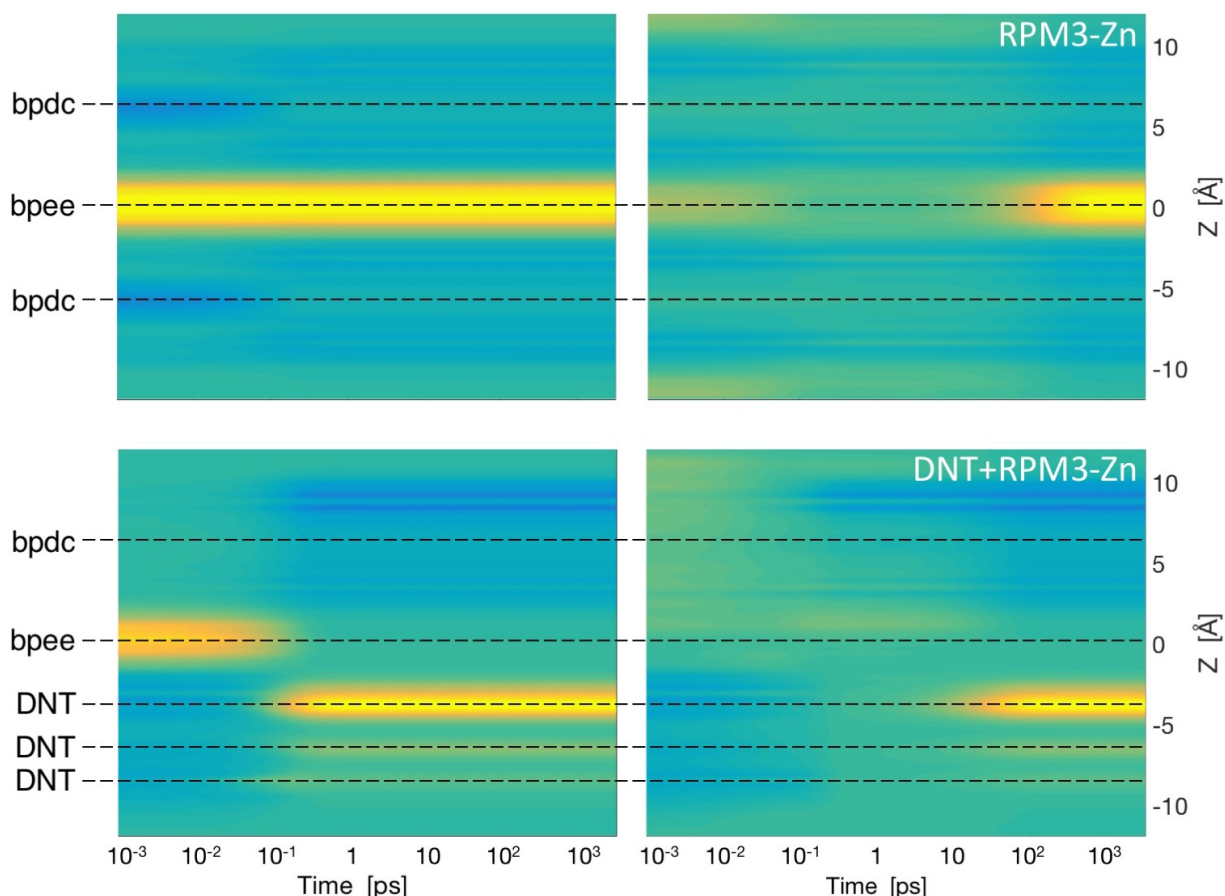


Figure S9. Electron and hole relaxation in real space along the z -axis of RPM3-Zn (top) and DNT+RPM3-Zn (bottom) for a lower energy transition at 340 nm/3.65 eV (left) and a higher energy transition at 260 nm/4.77 eV (right). Yellow indicates a gain of an electron, blue indicates a loss of an electron (i.e. hole), and green indicates no change in charge. The plots are obtained by integrating the charge density in the xy -plane and showing the result for all z values in the unit cell as a function of time. See Fig. 6 in the main manuscript for the alignment with the crystal structure.

* These authors contributed equally

† E-mail: thonhauser@wfu.edu

¹ G. Andreev, B. Jordanov, I. Juchnovski, and B. Schrader, *J. Mol. Struct.* **115**, 375 (1984).

² N. Nijem, H. Wu, P. Canepa, A. Marti, K. J. Balkus, T. Thonhauser, J. Li, and Y. J. Chabal, *J. Am. Chem. Soc.* **134**, 15201 (2012).

³ Z. Özhamam, M. Yurdakul, and Ş. Yurdakul, *J. Mol. Struct. Theochem* **761**, 113 (2006).

⁴ S. Mohr, T. Schmitt, T. Döpper, F. Xiang, M. Schwarz, A. Görling, M. A. Schneider, and J. Libuda, *Langmuir* **33**, 4178 (2017).